Room Temperature Trapping of Rhodopsin Photointermediates†

Sharon Sikora, Andrew S. Little, and T. Gregory Dewey*

Department of Chemistry, University of Denver, Denver, Colorado 80208

Received January 19, 1994; Revised Manuscript Received February 23, 1994®

ABSTRACT: By suspending bovine rhodopsin in trehalose–water glass films, it is possible to trap photostates in the light-activation process. Because of the unusually high vitrification temperature of trehalose–water mixtures, this trapping can be accomplished at room temperature. This allows for a facile investigation of the spectroscopic properties of rhodopsin's photointermediates. Depending on experimental conditions, it is possible to trap photolysis products that have visible absorbance spectra closely resembling the two different photointermediates, metarhodopsin I and metarhodopsin II. When rhodopsin is maintained in the native rod outer segment membrane, the photolysis product has the spectral properties of metarhodopsin I. Upon detergent solubilization, the photolysis product closely resembles metarhodopsin II. Ultraviolet circular dichroism spectra show that the metarhodopsin I product had no change in secondary structure compared with unbleached rhodopsin. The metarhodopsin II product did show a significant decrease in α-helical content. Resonance energy transfer was measured from extrinsic probes located on each of the cytoplasmic cysteine residues to the retinal in the trapped photoproducts. It is seen that these distances are the same for rhodopsin and metarhodopsin I while metarhodopsin II shows considerably shorter distances. Metarhodopsin II is intimately associated with the signal transduction process, and the present results suggest that large structural changes have occurred in the transition to this state. These results demonstrate the utility of room temperature trapping of photostates in trehalose–water glasses.

The photoreceptor rhodopsin is a member of the G-protein family of receptors and has been extensively studied. While the main biochemical features of visual transduction have been discovered, the mechanistic details of many of these coupled processes remain to be elucidated [for recent reviews, see Nathans (1992) and Chabre and Deterre (1989)]. After photoactivation, rhodopsin undergoes a series of complex thermal transitions between photostates. This system has a particular advantage in that the retinal chromophore acts as a spectroscopic indicator of the state of the protein. This provides a convenient monitor of the kinetics of the system and, in principle, will help unravel the mechanism of signal transduction. Two main approaches have been used to investigate the "bleaching" sequence of rhodopsin. They are low-temperature trapping of intermediates and rapid kinetic monitoring of spectral properties in solution. Unfortunately, these approaches have not provided a uniform picture of the photostates and mechanism of photoactivation of rhodopsin. While comparable kinetic and spectroscopic results are obtained when the early photointermediates are compared in ambient and low-temperature studies (Birge, 1992), it appears that a different bleaching mechanism is operative for the later stages of photobleaching (Lewis & Kliger, 1992). Thus, doubts have been raised concerning the physiological significance of these low-temperature approaches when important conformational steps late in the bleaching process are considered. Ambient solution-phase work has established that one of the late intermediates, M-II,[1] is responsible for G-protein activation. A large conformational change has been associated with this state upon transition from the M-I state [cf. Lamola et al. (1974) and Farahbakhsh et al. (1993)].

In the present work, it is demonstrated that rhodopsin photointermediates can be trapped at room temperature in trehalose–water glasses. Trehalose–water mixtures show an anomalously high vitrification temperature (Green & Angell, 1989), allowing glasses to be formed at room temperature. Trehalose possesses significantly higher glass transition temperatures than any other disaccharide or for glycerol at the same water content. This difference in transition temperature is largest when the water per glucose ring ratio is 1. Thus, a stoichiometric water–trehalose complex may be implicated in its anomalous behavior (Green & Angell, 1989). Trehalose is an unusual disaccharide that is found in high abundance in crytobiotic and anhydrobiotic organisms. Presumably its properties confer protection against low-temperature and/or arid conditions. There has been considerable interest in trehalose in the pharmaceutical industry as a stabilizing agent in the freeze-drying of biomaterials (Roser, 1991; Levine & Slade, 1992; Crowe et al., 1993a,b). It has been successfully used to preserve the functional integrity of the calcium ATPase in freeze-dried sarcoplasmic reticulum vesicles (Mouradian et al., 1984). The molecular details of the stabilization of biological samples in trehalose remain to be elucidated. However, a "water-replacement" hypothesis has been suggested in which trehalose hydrogen bonds to proteins and lipids in a manner similar to that of the water matrix (Roser, 1991). It is interesting to note that at ambient temperatures trehalose glasses will have a significant vapor pressure for water, while most carbohydrate glasses are hygroscopic. Thus, while trehalose may mimic the water matrix, water itself does not necessarily fit well into this matrix.

In the present work, it is shown that suspending rhodopsin in trehalose–water glasses allows the trapping of photolysis

† This work supported in part by NSF Grant MCB-900208.

* Author to whom correspondence should be addressed [telephone, (303)-871-3100; FAX, (303)-871-2254].

® Abstract published in *Advance ACS Abstracts,* April 1, 1994.

[1] Abbreviations: BSA, bovine serum albumin; CD, circular dichroism; ConA, concanavalin A; IAS, (iodoacetamido)salicylic acid; IA-NBD, *N,N'*-dimethyl-*N*-(iodoacetyl)-*N'*-(7-nitrobenz-2-oxa-1,3-diazol-4-yl)ethylenediamine; M-I, metarhodopsin I; M-II, metarhodopsin II; ROS, rod outer segments; SDS, sodium dodecyl sulfate.

0006-2960/94/0433-4454$04.50/0

products. Depending on solubilization conditions, an intermediate resembling M-I or M-II can be generated. This room temperature trapping allows for a facile exploration of the spectroscopy of these states. The visible absorbance and amide region CD spectra of these states are reported. Additionally, fluorescence resonance energy transfer has been measured from specifically labeled cysteine sites to the retinal in each of these states.

MATERIALS AND METHODS

Preparative Techniques. Dark adapted, frozen bovine retinas were purchased from Excel Co. (St. Louis, MO). Rod outer segments were purified by the procedure of Smith et al. (1975) and stored frozen in a 0.061 M K_2HPO_4, 0.039 M NaH_2PO_4, and 0.02 M NaCl buffer, pH 7.0, containing 45% (w/v) sucrose at −80 °C. All procedures, unless otherwise noted, were performed in darkness or under dim red light. Rod outer segments were covalently labeled with the fluorescent probes, IA-NBD or IAS. Before being labeled with IA-NBD, the sucrose buffer was removed by two successive centrifugations and resuspended in 0.067 M NaH_2PO_4 buffer, pH 6.5. Freshly prepared stock IA-NBD solution (0.025 M) in acetonitrile was added to the ROS, and the mixture was incubated overnight at room temperature. The molar ratio of IA-NBD to rhodopsin in the incubation mixture was 30:1. IAS labeling involved suspending ROS in 0.2 M KH_2PO_4, pH 7.0. A 0.01 M stock solution of IAS was prepared and stored at 4 °C. The molar ratio of IAS to rhodopsin in the incubation mixture was 18:1. The reaction mixture was incubated overnight at room temperature. Labeled ROS were washed thoroughly with their respective buffers.

Labeled ROS were either purified or treated with BSA to remove excess label. Purified rhodopsin was prepared using a small (1 × 4 cm) concanavalin A (ConA)–agarose column as described previously (Litman, 1982). The column buffer contained 50 mM octyl glucoside and 100 mM NaH_2PO_4, pH 7.0. Labeled rod outer segments were solubilized in 1.0 mL of the column buffer and loaded onto the column. After 1 h, the column was washed with approximately 50 mL of the column buffer to remove residual unbound label. The purified rhodopsin was eluted with the column buffer containing 0.75 M methyl α-mannoside. Initially, 1 mL of the buffer was added to the column. After 3 h, 15 mL of eluant was collected into a 15-mL "Centriprep-10" container (Amicon Corp.) and concentrated to a volume of 2 mL. The sample was further concentrated to a volume of 0.2 mL using a "Centricon-10" concentrator. Excess label was also removed by incubating labeled rod outer segments with BSA. A 1 mg/mL BSA solution was prepared in either 0.067 M NaH_2PO_4, pH 6.5, for IA-NBD-labeled ROS or 0.2 M KH_2PO_4, pH 7.0, for IAS-labeled ROS. The sample was washed, resuspended in the BSA buffer, and incubated overnight on ice. After this incubation, the sample was washed four times with an additional 5 mL of the BSA buffer. Finally, the sample was suspended in 1.0 mL of buffer without BSA. This BSA wash removed nonspecifically bound label as evidenced by lack of a fluorescence band migrating at the front of a 15% SDS gel.

To ensure the specificity of the labeling, ROS were digested proteolytically with papain. Under fairly mild conditions, papain cleaves rhodopsin in native membranes into two main fragments, F1 and F2 (Papac et al., 1992). The labeled ROS were digested using an enzyme to substrate ratio of 1:8, and the reactions were terminated by the addition of iodoacetamide as described previously (Trayhurn et al., 1974; Pober, 1982). Following digestion and enzyme inhibition, ROS were pelleted, solubilized in 2% SDS, and run on 15% SDS gels. As can be seen in Figure 1, the F1 fragment, encompassing amino acid residues 1–240, is labeled by IA-NBD. Amino acids 328–348 are contained in the F2 fragment which is labeled by IAS. Both of these regions contain only one accessible cysteine for the label to covalently bind.

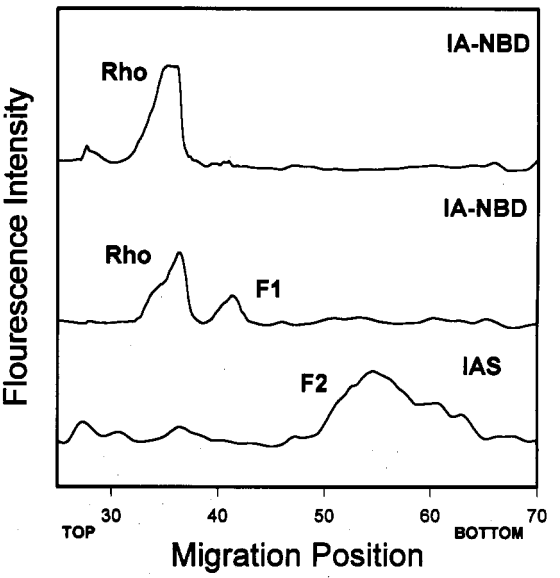

FIGURE 1: Densitometer tracing of a fluorescence image of an SDS gel containing papain proteolysis products of fluorescently labeled rhodopsin. (Top) IA-NBD-labeled rhodopsin. (Middle) Partial digest of IA-NBD-labeled rhodopsin. Fluorescence is contained in the F1 fragment with none appearing in the F2 fragment. (Bottom) Total digest of IAS-labeled rhodopsin. Fluorescence is entirely contained in the F2 fragment. Curves are displaced for better viewing.

Preparation of Trehalose–Water Glass Films. A 1.1 M stock solution of trehalose prepared in 0.067 M NaH_2PO_4 buffer, pH 6.5, for IA-NBD samples or 0.2 M KH_2PO_4 buffer, pH 7.0, for IAS samples was used throughout these experiments. Trehalose films containing ROS were prepared by centrifuging approximately 1 mg of protein and resuspending the pellet in 0.125 mL of the stock trehalose solution. For absorbance and fluorescence measurements, films were prepared on glass slides. For ultraviolet circular dichroism measurements, as a matter of convenience films were prepared on the outer surface of quartz cells. In either case, the trehalose/protein solution was added dropwise to the surface. The solution was allowed to dry undisturbed over a stream of nitrogen. Purified rhodopsin trehalose films were prepared in a similar manner. In this case, 0.2 mL of stock trehalose was added to an equal volume of purified rhodopsin.

Circular Dichroism and Absorbance Measurements. All CD measurements were performed on a Jasco J-500C spectropolarimeter. For experiments involving trehalose films, the CD cell was moved to within 2 cm of the photomultiplier tube to minimize light scattering artifacts. In these experiments, a trehalose-buffer blank was prepared on a quartz CD cell. Solution samples were placed in a 1-cm CD cell.

All absorbance measurements were taken on a Milton Roy Spectronic 3000 array spectrophotometer. Samples were bleached in the cell compartment of the spectrometer, ensuring identical alignment of the sample for the bleached and unbleached spectrum. Samples were bleached by exposure to a portable light source for 1 h. For trehalose film experiments, a trehalose-buffer blank was prepared on glass slides and a baseline was established. Absorbance spectra were obtained for the unbleached, M-I, and M-II photointermediates.

Table 1: Fluorescence Resonance Energy Transfer Results

condition	K^a	R_0 (Å)	$J \times 10^{14}$ (cm^3 M^{-1})	R (Å)
Labeling of F2 Fragment with IAS				
unbleached, purified rhodopsin in solution		27.6	8.7	34.8
unbleached ROS in solution		30.1	16.3	31.7
M-II, purified rhodopsin in solution	0.88	24.1	4.1	27.9
M-II, ROS in solution	1.23	20.5	2.3	23.8
M-I, ROS in trehalose film	1.04	30.3	17.4	32.4
M-II, purified rhodopsin in trehalose film	0.82	24.1	4.1	26.9
Labeling of F1 Fragment with IA-NBD				
unbleached, purified rhodopsin in solution		39.3	1.8	38.2
unbleached ROS in solution		38.5	1.3	42.0
M-I, ROS in trehalose film	1.12	37.6	1.1	43.6

[a] Ratio of fluorescence intensity of photolyzed and unbleached samples; see eq 3.

Fluorescence Measurements. Quantum yields for IA-NBD and IAS were determined by the method of Chen (1967) using as standards fluorescein and quinine sulfate, respectively. The quantum yield for IAS excited at 318 nm is 0.025 and 0.14 for IA-NBD excited at 472 nm. Corrected fluorescence spectra were obtained at room temperature with a Spex Fluorolog 2 spectrofluorometer. Fluorescence emission was monitored at 404 nm for IAS and 536 nm for IA-NBD. Fluorescence measurements were obtained for both ROS and purified rhodopsin in solution and in trehalose–water glass films. The solution spectra were taken with an excitation bandwidth of 0.2 nm and an emission bandwidth of 6 nm. Front-face fluorescence measurements were used to obtain the film spectra with an excitation bandwidth of 6 nm and an emission bandwidth of 0.4 nm. To measure the fluorescence response in the M-II state in solution, samples were exposed for 20 s to a 150-W xenon arc lamp filtered with a 4-in. water cell. The fluorescence spectrum was measured immediately afterward. Spectral measurements were generally completed within 1 min of initial exposure to light. Fully bleached samples were formed by exposure to a light box for 2 h at room temperature. Under these conditions, rhodopsin was converted completely to opsin.

Fluorescence Resonance Energy Transfer. The characteristic Förster distance, R_0, for each of the donor–acceptor pairs used was determined from eq 1, where n is the refractive index of the medium, κ^2 is a geometric factor characterizing the relative orientations of the transition dipoles of the donor and acceptor, Q_D is the quantum yield of the donor, and J is an overlap integral determined from the donor's emission and acceptor's absorbance spectra.

$$R_0 = (9.79 \times 10^3 \text{ Å})(J\kappa^2 Q_D n^{-4})^{1/6} \quad (1)$$

The refractive index of water, 1.33, was used. The major source of error is due to uncertainties in the orientation factor. The value of κ^2 was taken to be $^2/_3$, which corresponds to the case of rapid rotational averaging of the donor and acceptor orientations. The overlap integral was calculated from the emission spectra of each bleached sample and the absorbance spectra which corresponds to the photointermediate under investigation. These calculated values are presented in Table 1. There is no overlap between IA-NBD and the M-II photointermediate.

RESULTS

Absorbance and CD Spectroscopy. Figure 2 shows the visible absorbance spectra of rhodopsin and bleached rhodopsin in trehalose–water films. Rhodopsin in ROS shows an absorbance spectrum with a maximum at 498 nm that is virtually identical to the spectrum obtained in aqueous solution.

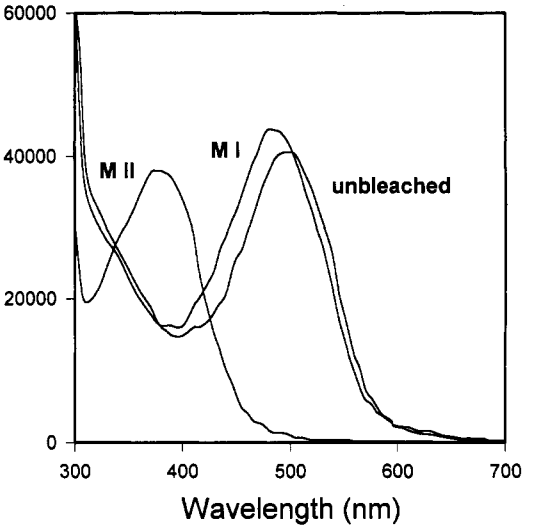

FIGURE 2: Absorbance spectra of rhodopsin in trehalose–water glass. The unbleached sample and photolysis product M-I are for rhodopsin in ROS. The photolysis product M-II is for detergent-solubilized ROS. Extinction coefficients were calculated assuming a value of 40 600 M^{-1} cm^{-1} for unbleached rhodopsin.

Upon bleaching, the absorbance maximum shifts to 480 nm, giving a spectrum comparable to that expected for the M-I photointermediate. Low-temperature trapping gives a 478-nm peak for the M-I state (Yoshizawa & Shichida, 1982), and an identical maximum was obtained with time-resolved absorbance measurements at room temperature (Applebury, 1984). Also shown in Figure 2 is the photolysis product spectrum for detergent-solubilized purified rhodopsin. It has an absorbance maximum at 380 nm as compared with the 378-nm maximum observed for the M-II state in the above-mentioned, low-temperature trapping and kinetic measurements. Thus, the photolysis product in the glass can be controlled merely by detergent solubilization. Since the trehalose–water glass environment may alter the kinetics and mechanism of rhodopsin photolysis, these results alone do not prove the trapping of M-I and M-II states identical to that occurring in aqueous solution. However, they are very suggestive that indeed this has been done. A full identification of these states will require additional spectroscopic and kinetic evidence. For simplicity these photolysis products will be referred to as M-I and M-II states.

In addition to the absorbance spectrum, the CD spectrum of the amide backbone region was measured. The unbleached ROS showed a spectrum (see Figure 3) characteristic of a protein with high α-helical content. Although the molar ellipticity is not readily determined for this sample, the shape of the spectrum closely resembles that for rhodopsin in aqueous

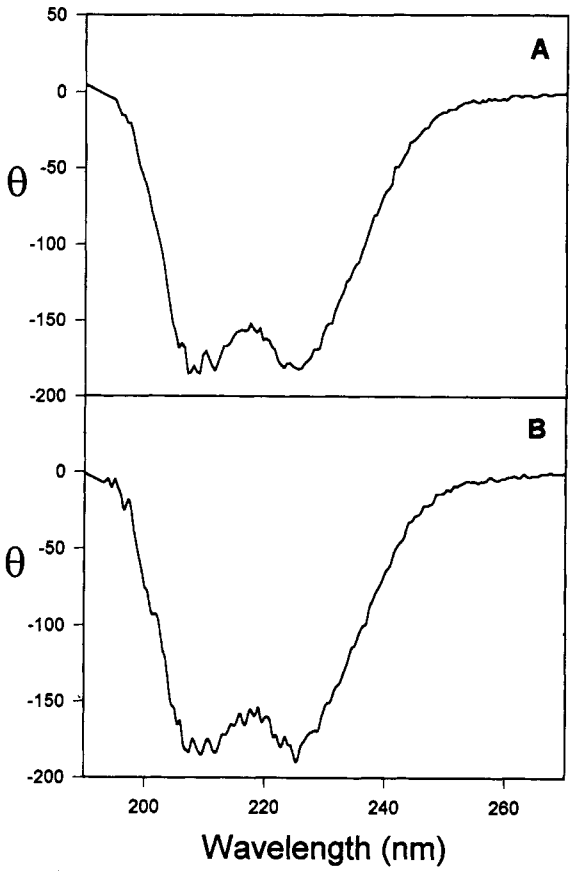

FIGURE 3: Circular dichroism spectra for rhodopsin in trehalose–water glass. Ellipticity is in arbitrary units. The sample is rhodopsin in ROS (A) and its photolysis product M-I (B).

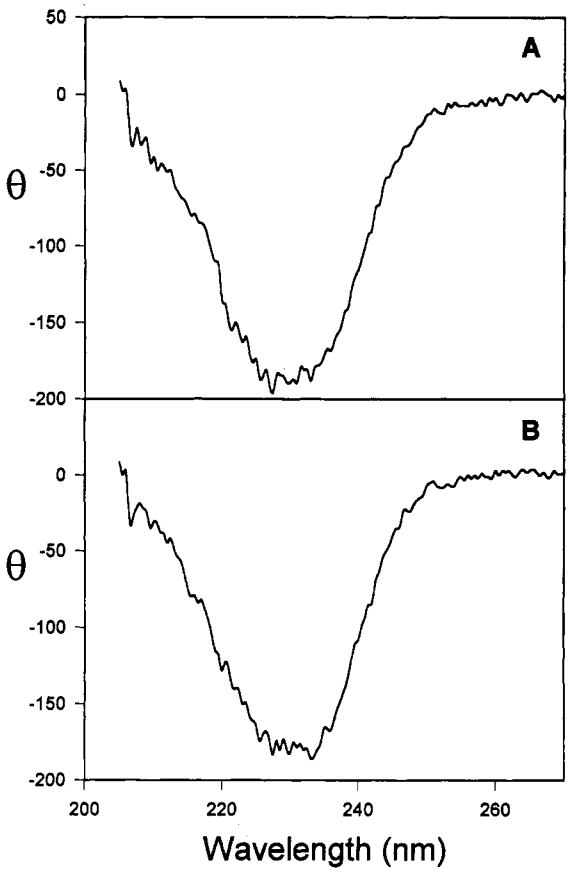

FIGURE 4: Circular dichroism spectra for rhodopsin in trehalose–water glass. Ellipticity is in arbitrary units. The sample is rhodopsin in detergent-solubilized ROS (A) and its photolysis product M-II (B).

solutions [cf. Stubbs et al. (1976)], suggesting that the trehalose–water glass has not greatly affected the protein's secondary structure. The photolysis to the M-I state showed no change in the CD spectrum (Figure 3) and indicates that major changes in conformation have not occurred during the transition from rhodopsin to M-I. A similar result was obtained with the CD of low-temperature, trapped lumirhodopsin (Ebrey & Yoshizawa, 1973). Figure 4 shows the amide CD for detergent-solubilized ROS. This spectrum has a large negative ellipticity at 222 nm, indicative of a high α-helical content. However, it is distorted and the double peak structure obtained for a pure α-helix is largely lost. Detergent-solubilized rhodopsin in aqueous solution shows a spectrum closer to that in Figure 3 than in Figure 4 [cf. Stubbs et al. (1976)]. Thus, there may be some alteration in secondary structure for solubilized rhodopsin in trehalose–water glasses. The photolysis product of this sample (Figure 4) shows a significant decrease in the negative CD peak. Bleached rhodopsin in aqueous solution also shows a decrease in ellipticity (Stubbs et al., 1978). These results are indicative of a significant change in secondary structure between unbleached, solubilized rhodopsin and rhodopsin in the putative M-II state.

Fluorescence Labeling and Resonance Energy Transfer. There are 10 cysteines in rhodopsin. Two are involved in a disulfide bridge and two are palmitoylated. Of the remaining six, only two (Cys-140 and Cys-316) are on the cytoplasmic side of the protein and are accessible to sulfhydryl modification in ROS. The site of labeling of IAS has been established to be on Cys-316 (McDowell & Griffith, 1978). The proteolysis of rhodopsin using papain results in two major fragments, F1 and F2 (Pober, 1982). The larger fragment, F1, contains the Cys-140 site while Cys-316 is in the small F2 fragment. Figure 1 shows an SDS–polyacrylamide gel of the papain proteolysis product of IAS-labeled rhodopsin. As can be seen, all the fluorescence is restricted to the F2 fragment, as expected for exclusive labeling of Cys-316. Interestingly, reaction of rhodopsin with IA-NBD results in exclusive labeling of the F1 fragment (see Figure 1). Thus, the IA-NBD site is tentatively assigned as Cys-140.

Fluorescence resonance energy transfer was measured from each of these cysteine sites to the retinal chromophore. The distance from the respective cysteine to the retinal was measured in solution by determining the efficiency, E, of energy transfer. This is given by

$$E = 1 - \frac{Q_{DA}}{Q_D} = \frac{R_o^6}{R^6 + R_o^6} \quad (2)$$

where Q_{DA} and Q_D are the steady-state fluorescence in the presence and absence of donor and R is the distance between donor (IA-NBD or IAS) and acceptor (rhodopsin-bound retinyl). For measurements to retinal in unbleached rhodopsin, Q_{DA} is taken as the fluorescence of the unbleached state and Q_D is the fully bleached or opsin state. Although bleaching results in a retinyl moiety that can still act as an energy-transfer acceptor, in the opsin state the retinal will dissociate from the protein and diffuse far from the fluorescent donors. If it is assumed that the dissociated retinal resides in the ROS membrane, a simple estimate shows that negligible energy transfer will occur from the cysteines to acceptors distributed at low density in the membrane. Table1 shows the fluorescent parameters and distances determined for the two different labeling sites.

The energy transfer was also measured in films and to the kinetically resolved M-II state in solution. These situations differ from that discussed above in that after photolysis the retinyl does not leave the protein. Since significant energy transfer can occur to these product retinyl states, the parameter Q_D cannot be unambiguously determined. Consequently, our analysis will be based on transfer to both the initial (unbleached) and final photolysis states. The ratio of fluorescence intensities, K, is given by

$$K = \frac{Q_{DA,p}}{Q_{DA,i}} = \frac{Q_{DA,p}/Q_{D,p}}{Q_{DA,i}/Q_{D,i}} = \frac{(1 + R_{o,p}^6/R_p^6)^{-1}}{(1 + R_o^6/R_i^6)^{-1}} \quad (3)$$

where the subscripts p and i represent the photolysis product and initial states, respectively, and eq 2 was used to obtain the second equality in eq 3. The working assumption is that all observed fluorescence changes are dominated by energy-transfer effects, i.e., $Q_{D,i} = Q_{D,p}$. Equation 3 can be manipulated to allow the determination of R_p, the distance from the cysteine label to the retinyl in the photolysis product. This gives

$$R_p = \frac{R_{o,p}}{\{K^{-1}(1 + (R_{o,i}/R_i)^6) - 1\}^{1/6}} \quad (4)$$

The distances obtained for transfer to unbleached retinal provide a value for R_i and allow the calculation of the cysteine to retinal distance, R_p, in the M-I or M-II state. Again, the parameters for these experiments and distances are given in Table 1. Distances determined by resonance energy transfer measurements commonly have errors of 10% associated with them as a result of uncertainty in the characteristic Förster distance. Bearing this in mind, it is seen in Table 1 that the distance changes in the transition from rhodopsin to metarhodopsin I are not significant. However, the apparent change in distance for the rhodopsin to M-II transition is very large, indicative of a significant structural change. It is also worth noting that the distances in the M-II state in the film and in solution are essentially the same.

DISCUSSION

In this work it was shown that photolysis products of rhodopsin can be trapped at room temperature in trehalose–water glasses. It is particularly convenient that the specific product formed can be dictated by the sample preparation conditions. For rhodopsin in ROS, the product resembles the M-I photointermediate. When the preparation is solubilized, photolysis yields a product with spectral properties similar to those of the M-II state. Characterization of the conformational properties of these states by CD spectroscopy and resonance energy transfer indicates that structurally the M-I state is very similar to rhodopsin. Significant changes occur in the transition to the M-II state, and these are indicative of a large conformational transition. This result is not unexpected as the M-II state is the one that activates G-protein and, therefore, must be structurally different from the other states. This large structural change in M-II provides a possible explanation for the environmental sensitivity of trapping in the glasses. Membrane-bound rhodopsin embedded in a glass matrix is presumably in a more constrained environment. It has both the lipid membrane and surrounding glass matrix confining it. Solubilized protein has the membrane dissolved away and is coated with detergent. The detergent–glass matrix interface may not be rigid because the trehalose has limited sites in which to hydrogen bond. This could afford increased flexibility for the protein. Thus, higher barriers to large conformational rearrangements will exist for the membrane-bound protein, and it cannot proceed from M-I to M-II. This barrier must be lowered considerably upon solubilization, allowing the formation of metarhodopsin II.

The resonance energy transfer results indicate that the distance from retinal to Cys-140 or Cys-316 decreases by as much as 10 Å upon forming the M-II state. Certainly these are very large effects for a protein conformational change to accommodate. Similar large changes in resonance energy transfer to the retinal have been observed for photointermediates of bacteriorhodopsin (Hasselbacher & Dewey, 1986; Hasselbacher et al., 1986). Distance changes measured by resonance energy transfer in such systems should be considered as "apparent" changes because of the high degree of orientation of the retinal. Invariably, retinal translation will be strongly coupled to rotation. Thus, even a small movement may result in strong orientational effects that will affect the characteristic Förster distance, R_o. This can readily give an appearance of a distance change. As a rule of thumb, orientation effects on R_o result in a 10–20% error in the distances. Thus, at the extreme of the error limits virtually the entire observed change could be accommodated by a rotation of the retinal. Regardless of the source of the apparent distance change, the results indicate that a major structural rearrangement has occurred in the M-II state compared with the unbleached state. This change was not seen in the M-I state. These results are further corroborated by the circular dichroism results.

It is obviously of great utility for kinetic and spectroscopic investigations to be able to trap individual states at room temperature. However, these results raise a number of interesting and important questions. Will states trapped at room temperature in a glass matrix resemble the room temperature solution states or the low-temperature glass states? The room temperature glasses provide structural constraints similar to those of the low-temperature matrices. However, thermal effects on local structures via rotational and vibrational effects will more closely resemble those in the solution phase. Another important question is whether the reaction mechanism for photolysis changes in the room temperature matrix. Room temperature matrices may facilitate the observation of fast intermediates relevant to the solution-phase mechanism. These issues are currently being investigated.

ACKNOWLEDGMENT

We thank Dr. Robert Hurturbise for introducing us to the properties of trehalose.

REFERENCES

Applebury, M. L. (1984) *Vision Res. 24*, 1445–1454.
Birge, R. (1990) *Biochim. Biophys. Acta 1016*, 293–327.
Chabre, M., & Deterre, P. (1989) *Eur. J. Biochem. 179*, 255–266.
Chen, R. (1967) *Anal. Biochem. 19*, 374–387.
Crowe, J. H., Crowe, L. M., & Carpenter, J. F. (1993a) *BioPharm 6*, 28–37.
Crowe, J. H., Crowe, L. M., & Carpenter, J. F. (1993b) *BioPharm 6*, 40–43.
Ebrey, T. G., & Yoshizawa, T. (1973) *Exp. Eye Res. 17*, 545–556.
Farahbakhsh, Z. T., Hideg, K., & Hubbell, W. L. (1993) *Science 262*, 1416–1419.
Green, J. L., & Angell, C. A. (1989) *J. Phys. Chem. 93*, 2880–2882.

Hasselbacher, C. A., & Dewey, T. G. (1986) *Biochemistry 25*, 6236–6243.
Hasselbacher, C. A., Preuss, D. K., & Dewey, T. G. (1986) *Biochemistry 25*, 668–676.
Lamola, A. A., Yamane, T., & Zipp, A. (1974) *Biochemistry 13*, 738–745.
Levine, H., & Slade, L. (1992) *Biopharm 5*, 36–40.
Lewis, J. W., & Kliger, D. S. (1992) *J. Bioenerg. Biomembr. 24*, 201–210.
McDowell, J. H., & Griffith, K. (1978) *Invest. Ophthal. Visual Sci. (Suppl.) 17*, 125.
Mouradian, R., Womersley, C., Crowe, L. M., & Crowe, J. H. (1984) *Biochim. Biophys. Acta 778*, 615–617.
Nathans, J. (1992) *Biochemistry 31*, 4923–4931.
Papac, D. L., Thornburg, K. R., Bullesbach, E. E., Crouch, R. K., & Knapp, D. R. (1992) *J. Biol. Chem. 267*, 16889–16894.
Pober, J. S. (1982) *Methods Enzymol. 81*, 236–239.
Roser, B. (1991) *BioPharm 4*, 47–53.
Stubbs, G. W., Smith, H. G., Jr., & Litman, B. J. (1976) *Biochim. Biophys. Acta 425*, 46–56.
Trayhurn, P., Mandel, P., & Virmaux, N. (1974) *FEBS Lett. 38*, 351–353.
Yoshizawa, T., & Shichida, Y. (1982) *Methods Enzymol. 81*, 333–353.